

# Evaluation of the Cray XT3 at ORNL: a Status Report

Sadaf R. Alam  
O. E. Bronson Messer

Jeffrey S. Vetter

Richard F. Barrett  
Richard T. Mills

Patrick H. Worley

Mark R. Fahey  
Philip C. Roth

Oak Ridge National Laboratory  
Oak Ridge, TN, USA 37831

{alamsr,rbarrett,faheymr,bronson,rmills,rothpc,vetter,worleyph}@ornl.gov

---

**Abstract** – Last year, Oak Ridge National Laboratory received delivery of a 5,294 processor Cray XT3. The XT3 is Cray’s third-generation massively parallel processing system. The system uses a single-processor node built around the AMD Opteron and uses a custom chip—called SeaStar—to provide interprocessor communication. In addition, the system uses a lightweight operating system on its compute nodes. This paper provides a status update since last year, including updated performance measurements for micro-benchmark, kernel, and application benchmarks. In particular, we provide performance results for strategic Department of Energy applications areas including climate, biology, astrophysics, combustion, and fusion. Our results, on up to 4096 processors, demonstrate that the Cray XT3 provides competitive processor performance, high interconnect bandwidth, and high parallel efficiency on a diverse application workload, typical in the DOE Office of Science.

---

## 1 Introduction

Computational requirements for many large-scale simulations and ensemble studies of vital interest to the Department of Energy (DOE) exceed what is currently offered by any U.S. computer vendor. As illustrated in the DOE Scales report [43] and the High End Computing Revitalization Task Force report [24], examples are numerous, ranging from global climate change research to combustion to biology.

Performance of the current class of high performance computer (HPC) architectures is dependent on the performance of the memory hierarchy, ranging from the processor-to-cache latency and bandwidth to the latency and bandwidth of the interconnect between nodes in a cluster, to the latency and bandwidth in accesses to the file system. With increasing chip clock rates and number of functional units per processor and the lack of corresponding improvements in memory access latencies, this dependency will only increase. Single processor performance, or the performance of a small system, is relatively simple to determine. However, given reasonable sequential performance, the metric of interest in evaluating the ability of a system to achieve multi-Teraop performance is scalability. Here, scalability includes the performance sensitivity to variation in both problem size and the number of processors or other computational resources utilized by a particular application.

ORNL has been evaluating these critical factors on several platforms that include the Cray X1 [2], the SGI Altix 3700 [18], and the Cray XD1 [20]. This report is a

status update to our ongoing use and evaluation of the Cray XT3 sited at ORNL.

## 2 Cray XT3 System Overview

The XT3 is Cray’s third-generation massively parallel processing system. It follows a similar design to the successful Cray T3D and Cray T3E [40] systems. As in these previous systems, the XT3 builds upon a single processor node, or processing element (PE). However, unlike the T3D and T3E, the XT3 uses a commodity microprocessor—the AMD Opteron—at its core. The XT3 connects these processors with a customized interconnect managed by a Cray-designed Application-Specific Integrated Circuit (ASIC) called SeaStar.

### 2.1 Processing Elements

As Figure 1 shows, each PE has one Opteron processor with its own dedicated memory and communication resource. The XT3 has two types of PEs: compute PEs and service PEs. The compute PEs are optimized for application performance and run a lightweight operating system kernel called Catamount. In contrast, the service PEs run SuSE Linux and are configured for I/O, login, network, or system functions.

The ORNL XT3 uses Opteron model 150 processors. This model includes an Opteron core, integrated memory controller, three 16b-wide 800 MHz HyperTransport (HT) links, and L1 and L2 caches. The Opteron core has three integer units and one floating point unit capable of two floating-point operations per cycle [4]. Because the processor core is clocked at 2.4

GHz, the peak floating point rate of each compute node is 4.8 GFlops.

The memory structure of the Opteron consists of a 64KB 2-way associative L1 data cache, a 64KB 2-way associative L1 instruction cache, and a 1MB 16-way associative, unified L2 cache. Each PE has 2 GB of memory but only 1 GB is usable with the kernel used for our evaluation. The memory DIMMs are 1 GB PC3200, Registered ECC, 18 x 512 mbit parts that support Chipkill. The peak memory bandwidth per processor is 6.4 GB/s. Also, the Opteron 150 has an on-chip memory controller. As a result, memory access latencies with the Opteron 150 are in the 50-60 ns range. These observations are quantified in Section 4.1.

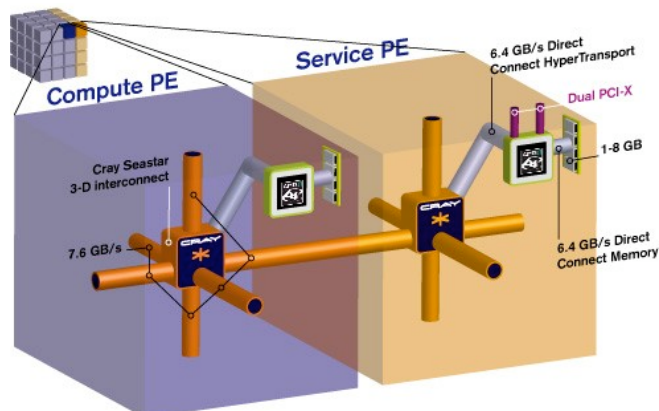


Figure 1: Cray XT3 Architecture (Image courtesy of Cray).

## 2.2 Interconnect

Each Opteron processor is directly connected to the XT3 interconnect via a Cray SeaStar chip (see Figure 1). This SeaStar chip is a routing and communications chip and it acts as the gateway to the XT3's high-bandwidth, low-latency interconnect. The PE is connected to the SeaStar chip with a 6.4 GB/s HT path. SeaStar provides six high-speed network links to connect to neighbors in a 3D torus/mesh topology. Each of the six links has a peak bandwidth of 7.6 GB/s with sustained bandwidth of around 4 GB/s. In the XT3, the interconnect carries all message passing traffic as well as I/O traffic to the system's Lustre parallel file system.

The ORNL Cray XT3 has 56 cabinets holding 5,212 compute processors and 82 service processors. Its nodes are connected in a three-dimensional mesh of size 14 x 16 x 24, with torus links in the first and third dimension.

## 2.3 Software

The Cray XT3 inherits several aspects of its systems software approach from a sequence of systems developed and deployed at Sandia National Laboratories: ASCI Red [34], the Cplant [10, 38], and Red Storm [9]. The XT3 uses a lightweight kernel operating system on its compute PEs, a user-space

communications library, and a hierarchical approach for scalable application start-up.

The XT3 uses two different operating systems: Catamount on compute PEs and Linux on service PEs. For scalability and performance predictability, each instance of the Catamount kernel runs only one single-threaded process and does not provide services like demand-paged virtual memory that could cause unpredictable performance behavior. Unlike the compute PEs, service PEs (i.e., login, I/O, network, and system PEs) run a full SuSE Linux distribution to provide a familiar and powerful environment for application development and for hosting system and performance tools.

The XT3 uses the Portals [11] data movement layer for flexible, low-overhead inter-node communication. Portals provide connectionless, reliable, in-order delivery of messages between processes. For high performance and to avoid unpredictable changes in the kernel's memory footprint, Portals deliver data from a sending process' user space to the receiving process' user space without kernel buffering. Portals supports both one-sided and two-sided communication models.

The primary math library is the AMD Core Math Library (ACML). It incorporates BLAS, LAPACK and FFT routines, and is optimized for high performance on AMD platforms.

## 3 Evaluation Overview

As a function of the Early Evaluation project at ORNL, numerous systems have been rigorously evaluated using important DOE applications. Recent evaluations have included the Cray X1 [17], the SGI Altix 3700 [18], and the Cray XD1 [20]. The primary goals of these evaluations are to 1) determine the most effective approaches for using the each system, 2) evaluate benchmark and application performance, both in absolute terms and in comparison with other systems, and 3) predict scalability, both in terms of problem size and in number of processors.

For comparison, performance data is also presented for the following systems:

- Cray X1 at ORNL: 512 Multistreaming processors (MSP), each capable of 12.8 GFlops/sec for 64-bit operations. Each MSP is comprised of four single streaming processors (SSPs). The SSP uses two clock frequencies, 800 MHz for the vector units and 400 MHz for the scalar unit. Each SSP is capable of 3.2 GFlops/sec for 64-bit operations. MSPs are fully connected within 16 MSP subsets, and are connected via a 2-D torus between subsets.
- Cray X1E at ORNL: 1024 Multistreaming processors (MSP), each capable of 18 GFlops/sec for 64-bit operations. Each MSP is comprised of four single streaming processors (SSPs). The SSP uses two clock frequencies, 1130 MHz for the vector units and 565 MHz for the scalar unit. Each SSP is

capable of 4.5 GFlops/sec for 64-bit operations. MSPs are fully connected within 32 MSP subsets, and are connected via a 2-D torus between subsets. This system is an upgrade of the original Cray X1 at ORNL.

- Opteron cluster at Combustion Research Facility/Sandia (CRF/S): 286 AMD 2.0GHz Opteron processors with 1GB of memory per processor. System is configured as 143, 2-way SMPs with an Infiniband interconnect.
- Cray XD1 at ORNL: 144 AMD 2.2GHz Opteron 248 processors with 4GB of memory per processor. System is configured as 72, 2-way SMPs with Cray's proprietary RapidArray interconnect fabric.
- Earth Simulator: 640 8-way vector SMP nodes and a 640x640 single-stage crossbar interconnect. Each processor has 8 64-bit floating point vector units running at 500 MHz.
- SGI Altix at ORNL: 256 Itanium2 processors and a NUMalink switch. The processors are 1.5 GHz Itanium2. The machine has an aggregate of 2 TB of shared memory.
- SGI Altix at the National Aeronautic and Space Administration (NASA): Twenty Altix 3700 nodes, where each node contains 512 Itanium2 processors with SGI's NUMaflex interconnect. We used two such nodes, both Altix 3700 BX2 nodes with 1.6 GHz processors, connected by a NUMalink4 switch and running as a single global shared memory system.
- HP/Linux Itanium-2 cluster at the Pacific Northwest National Laboratory (PNNL): 1960 Itanium-2 1.5 GHz processors. System is configured as 980, 2-way SMP nodes with a Quadrics QsNetII interconnect. 574 compute nodes have 8GB of memory and 366 compute nodes have 6 GB of memory.
- IBM p690 cluster at ORNL: 27 32-way p690 SMP nodes and an HPS interconnect. Each node has two HPS adapters, each with two ports. The processors are the 1.3 GHz POWER4.
- IBM p575 cluster at the National Energy Research Supercomputer Center (NERSC): 122 8-way p575 SMP nodes (1.9 GHz POWER5 processors) and an HPS interconnect with 1 two-link adapter per node.
- IBM SP at NERSC: 184 Nighthawk(NH) II 16-way SMP nodes and an SP Switch2. Each node has two interconnect interfaces. The processors are the 375MHz POWER3-II.
- IBM Blue Gene/L at ANL: a 1024-node Blue Gene/L system at Argonne National Laboratory. Each Blue Gene/L processing node consists of an ASIC with two PowerPC processor cores, on-chip memory and communication logic. The total processing power per node is 2.8 GFlops per processor or 5.6 GFlops per processing node. Experiments were run in either 'virtual node' (VN) mode, where both processors in the BG/L node

were used for computation, or Co-Processor (CP) mode, where one processor was used for computation and one was used for communication.

## 4 Micro-benchmarks

The objective of micro-benchmarking is to characterize the performance of the specific architectural components of the platform. We use both standard benchmarks and customized benchmarks. The standard benchmarks allow consistent historical comparisons across platforms. The custom benchmarks permit the unique architectural features of the system (e.g., global address space memory) to be tested with respect to the target applications.

Traditionally, our micro-benchmarking focuses on the arithmetic performance, memory-hierarchy performance, task and thread performance, message-passing performance, system and I/O performance, and parallel I/O. However, because the XT3 has a single processor node and it uses a lightweight operating system, we focus only on these areas:

- Arithmetic performance, including varying instruction mix, identifying what limits computational performance.
- Memory-hierarchy performance, including levels of cache and shared memory.
- Message-passing performance, including one-way (ping-pong) messages, message exchanges, and collective operations (broadcast, all-to-all, reductions, barriers), message-passing hotspots, and the effect of message passing on the memory subsystem.

### 4.1 Memory Performance

The memory performance of current architectures is a primary factor for performance on scientific applications. Table 1 illustrates the differences in measured memory bandwidth for one processor on the triad STREAM benchmark. The very high bandwidth of the Cray X1 MSP clearly dominates the other processors, but the Cray XT3's Opteron has the highest bandwidth of the other microprocessor-based systems. The XT3 bandwidth we report was measured in April 2006 using the PGI 6.1 compiler. The observed bandwidth is sensitive to compiler, compiler flags, and data placement. A STREAM Triad bandwidth of 5.1 GB/s was measured on the ORNL XT3 using the Pathscale compiler, but that compiler is not currently supported on the ORNL XT3.

**Table 1: STREAM Triad Performance.**

System	Triad Bandwidth (GB/s)
Cray XT3 (ORNL)	4.9
Cray XD1 (ORNL)	4.1
Cray X1E MSP (ORNL)	23.1
IBM p690 (ORNL)	2.1
IBM POWER5 (NERSC)	4.0

SGI Altix (ORNL)	3.7
------------------	-----

As discussed earlier, the choice of the Opteron model 150 was motivated in part to provide low access latency to main memory. As Table 2 shows, our measurements revealed that the Opteron 150 has lower latency than the Opteron 248 configured as a 2-way SMP in the XD1. Furthermore, it has considerably smaller latency than either the POWER4 or the Intel Xeon, which both support multiprocessor configurations (and hence must include logic for maintaining cache coherence that contributes to the main memory access latency).

**Table 2: Latency to Main Memory.**

Platform	Measured Latency to Main Memory (ns)
Cray XT3 / Opteron 150 / 2.4 GHz	51.41
Cray XD1 / Opteron 248 / 2.2 GHz	86.51
IBM p690 / POWER4 / 1.3 GHz	90.57
Intel Xeon / 3.0 GHz	140.57

The memory hierarchy of the XT3 compute node is obvious when measured with the CacheBench tool [36]. Figure 2 shows that the system reaches a maximum of approximately 9 GB/s when accessing vectors of data in the L2 cache. When data is accessed from main memory, the bandwidth drops to about 3 GB/s.

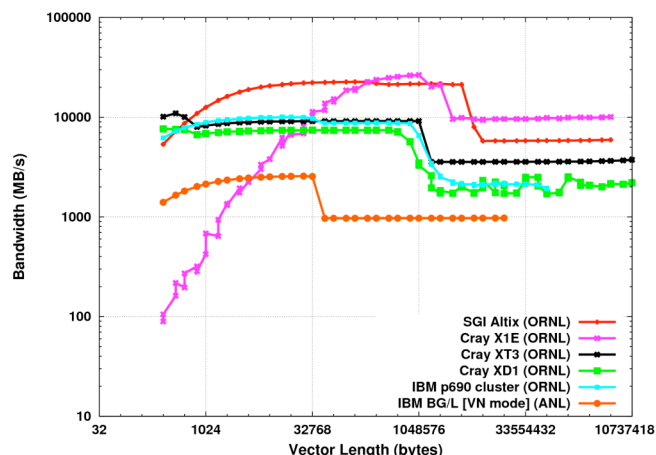


**Figure 2: CacheBench read results for a single XT3 compute node.**

## 4.2 Scientific Operations

We use a collection of micro-benchmarks to characterize the performance of the underlying hardware, compilers, and software libraries for common operations in computational science. The micro-benchmarks measure computational performance, memory hierarchy performance, and inter-processor communication. Figure 3 compares the double-precision floating point performance of a matrix multiply (DGEMM) on a single processor using the vendors' scientific libraries. In our tests, the XT3 with the ACML 3.0 library achieved its highest DGEMM performance for matrices of order 1600; the observed

performance was 4396 MB/s, approximately 91.6% of the Opteron 150's peak.

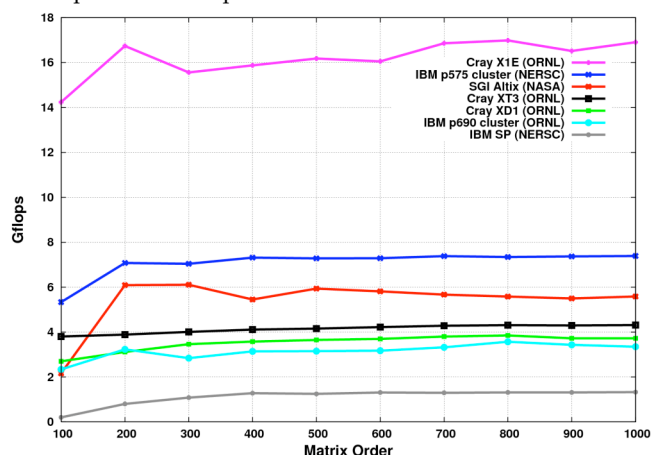


**Figure 3: Performance of Matrix Multiply.**

Fast Fourier Transforms are another operation important to many scientific and signal processing applications. Figure 4 plots 1-D FFT performance using the vendor library (-lacml, -lscs, -lsci or -lessl), where initialization time is not included. The XT3's Opteron is outperformed by the SGI Altix's Itanium2 processor for all vector lengths examined, but does better than the Power4 processor in the p690 and better than the X1E for short vectors.

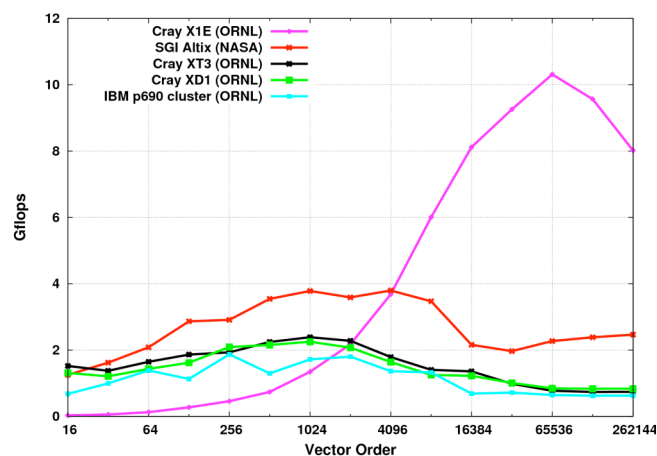


**Figure 4: Performance of 1-D FFT using vendor libraries.**

In general, our micro-benchmark results suggest *performance stability* from the XT3 compute nodes, in that they may not be the best performing for any of the micro-benchmarks but they perform reasonably well on all of them.

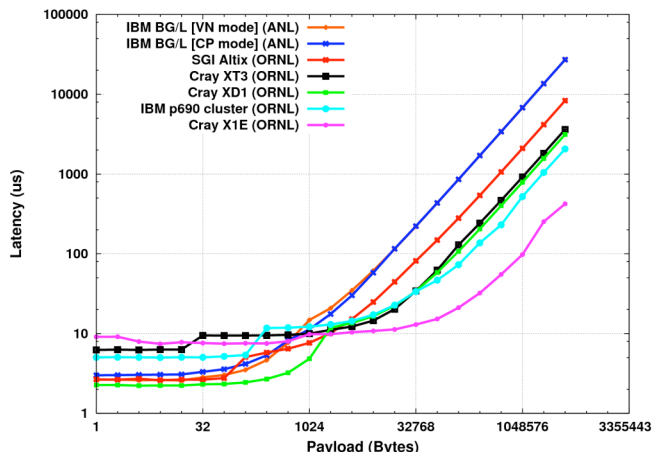


Figure 5: IMB PingPong benchmark latency.

### 4.3 MPI

Because of the predominance of the message-passing programming model in contemporary scientific applications, examining the performance of message-passing operations is critical to understanding a system's expected performance characteristics when running full applications. Because most applications use the Message Passing Interface (MPI) library [41], we evaluated the performance of each vendor's MPI implementation. For our evaluation, we used the Intel MPI Benchmark (IMB) suite, version 2.3. In general, the MPI performance of the Cray XT3 was observed to be unexceptional compared to the other systems we tested, and was even observed to be significantly worse for some collectives with small messages.

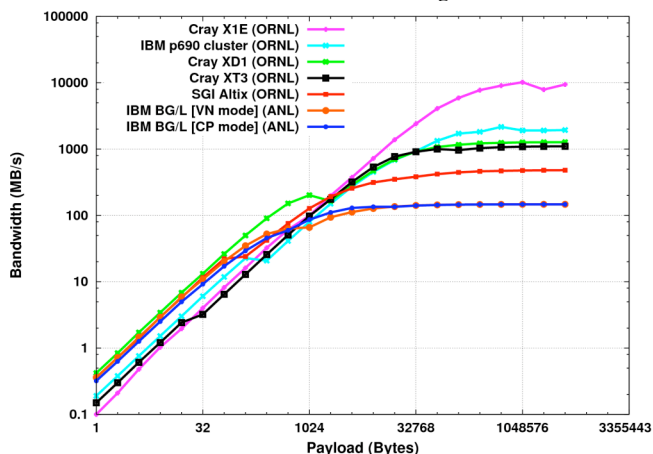


Figure 6: IMB PingPong bandwidth.

Figure 5 and Figure 6 show the latency and bandwidth, respectively, for the IMB PingPong benchmark. Like all IMB benchmarks that report both bandwidth and latency, the PingPong bandwidth is calculated from the measured latency so the two figures are different perspectives on the same data. The null message latency on the XT3 was observed to be just over 6 microseconds, and the maximum

bandwidth 1104 GB/s. The XT3 performance was among the worst of the systems tested for messages smaller than 1KB, and rises only to the middle of the pack for larger messages. These results were collected in April 2006; the latencies are 3% to 5% higher than the latency we measured in November 2005 for short messages, but the maximum bandwidth is very nearly the same. Because the operating system, MPI implementation, and SeaStar firmware have been modified since November 2005, we cannot say with certainty where to attribute the additional overhead.

Figure 7 and Figure 8 show the latency and bandwidth, respectively, for the Intel Exchange benchmark on the largest number of MPI tasks we could obtain across all of our test systems. The Exchange benchmark is intended to represent the behavior of a code performing boundary-exchange communication. In this benchmark, each task performs one-dimensional nearest-neighbor communication using MPI\_Isend, MPI\_Recv, and MPI\_Waitall. The benchmark program measures the time required to send data to its left and right neighbor and to receive data sent by those neighbors. Similar to the IMB PingPong benchmark, bandwidth is computed from the observed latency but considers that each process sends two messages and receives two messages. Because this benchmark measures latency and bandwidth using point-to-point MPI operations when all MPI tasks are communicating, it is a more realistic test of a system's MPI performance than the PingPong benchmark for a large class of scientific applications. For the largest number of MPI tasks we tested on the XT3 (4096), we observed an average latency of 11.99 microseconds for 4-byte messages and a maximum bandwidth of 1262 MB/s for 512KB messages. The Cray XD1 showed the best Exchange performance of the systems we tested for messages smaller than 2KB, whereas we observed the best performance for larger messages with the Cray X1E.

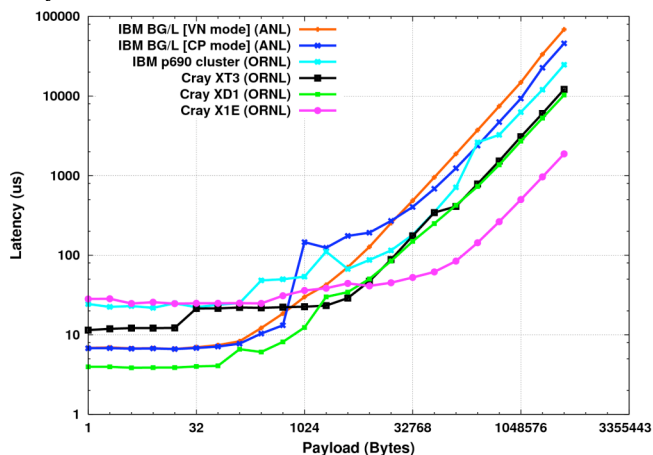


Figure 7: IMB Exchange benchmark latency at 128 tasks.

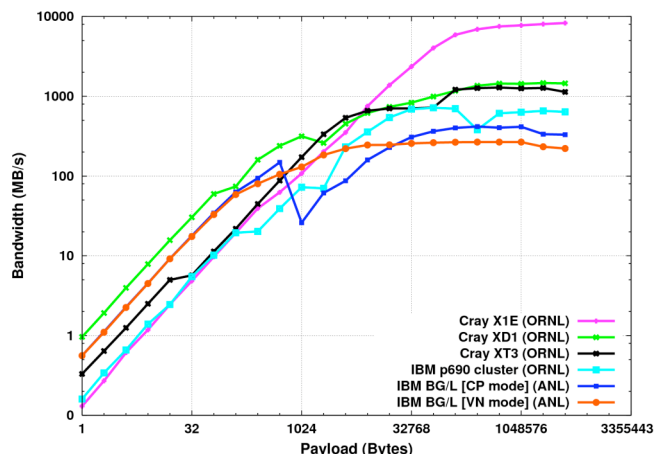


Figure 8: IMB Exchange benchmark bandwidth at 128 tasks.

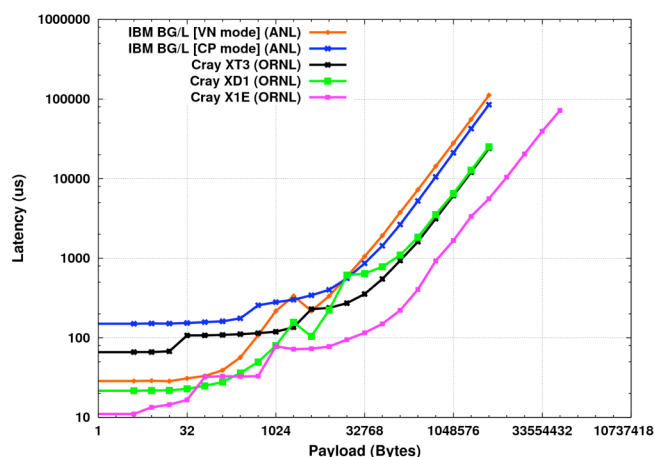


Figure 9: IMB Allreduce benchmark latency at 128 tasks.

The MPI\_Allreduce operation is particularly important for several DOE simulation applications; for some applications, it is used several times within each simulation timestep. Its blocking semantics also require that all tasks wait for its completion before continuing, so the latency of this operation is an important factor with regard to application scalability. The IMB Allreduce benchmark tests the latency of the MPI\_Allreduce operation. (The IMB developers do not consider bandwidth to be a well-defined concept for MPI collective operations, so the IMB collective benchmarks including Allreduce do not report a bandwidth measurement.) Our IMB Allreduce latency results are shown in Figure 9. The Cray XT3 Allreduce performance is the worst among the systems tested for small messages, whereas the Cray XD1 and X1E performed very well for small messages and the X1E was superior for messages larger than 2KB.

## 5 Applications

Insight into the performance characteristics of low-level operations is important to understand overall system performance, but because a system's behavior

when running full applications is the most significant measure of its performance, we also investigate the performance and efficiency of full applications relevant to the DOE Office of Science in the areas of global climate, fusion, chemistry, and bioinformatics. The evaluation team worked closely with principal investigators leading the Scientific Discovery through Advanced Computing (SciDAC) application teams to identify important applications.

### 5.1 CAM

The Community Atmosphere Model (CAM) is a global atmosphere model developed at the National Science Foundation's National Center for Atmospheric Research (NCAR) with contributions from researchers funded by DOE and by NASA [14, 15]. CAM is used in both weather and climate research. In particular, CAM serves as the atmospheric component of the Community Climate System Model (CCSM) [1, 7]. As a community model, it is important that CAM run efficiently on different architectures, and that it be easily ported to and optimized on new platforms. CAM contains a number of compile-time and runtime parameters that can be used to optimize performance for a given platform, problem or processor count. When benchmarking with CAM it is important that the code be optimized to approximately the same level as for a production run, but no more. For example, production usage requires that the results be invariant to the number of processors used. This "reproducibility" requirement can disallow some compiler optimizations.

CAM is a mixed-mode parallel application code, using both MPI [41] and OpenMP protocols [16]. CAM is characterized by two computational phases: the dynamics, which advances the evolution equations for the atmospheric flow, and the physics, which approximates subgrid phenomena such as precipitation processes, clouds, long- and short-wave radiation, and turbulent mixing [14]. Control moves between the dynamics and the physics at least once during each model simulation timestep. The number and order of these transitions depend on the numerical algorithm in the dynamics.

CAM includes multiple *dynamical cores (dycores)*, one of which is selected at compile-time. Three dycores are currently supported: the spectral Eulerian solver from CCM [28], a spectral semi-Lagrangian solver [45], and a finite volume semi-Lagrangian solver [30]. The three dycores do not use the same computational grid. An explicit interface exists between the dynamics and the physics, and the physics data structures and parallelization strategies are independent from those in the dynamics. A dynamics-physics coupler moves data between data structures representing the dynamics state and the physics state.

For our evaluation we ported and optimized CAM versions 3.0p1 and 3.1, available for download from <http://www.cesm.ucar.edu/>, as described in Worley [46].

We used two different benchmark problems. The first uses the spectral Eulerian dycore with CAM 3.0p1, a 128×256 (latitude × longitude) horizontal computational grid covering the sphere, and 26 vertical levels. This problem, which is referred to as T85L26, is a common production resolution used with the CCSM. The second benchmark uses the finite volume (FV) dycore with CAM 3.1, a 361×576 horizontal computational grid, and 26 vertical levels. The CCSM community is currently transitioning from the spectral Eulerian dycore to the FV dycore in production runs. This problem resolution, referred to as the “D-grid,” is much larger than is envisioned for near-term production climate runs, but represents a resolution of interest for the future.

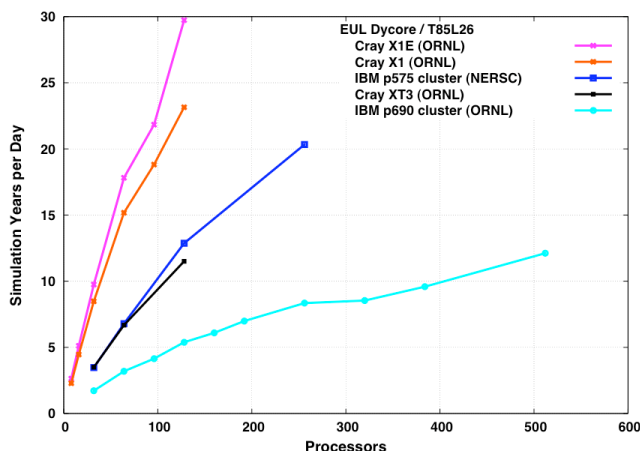


Figure 10: Platform comparisons using CAM T86L26 benchmark.

Figure 10 shows a platform comparison of CAM throughput for the T85L26 benchmark problem. The spectral Eulerian dycore supports only a one-dimensional latitude decomposition of the computational grid, limiting MPI parallelism to 128 processes for this computational grid. OpenMP can be used to exploit additional processors, but the XT3 cannot take advantage of this. By these results, the X1E is 2.5 times faster than the XT3 and the XT3 is 2.1 times faster than the p690 cluster for the same number of processors. Performance on the XT3 and the p575 cluster are similar for small processor counts. OpenMP parallelism gives the p575 cluster an advantage for large processor counts. While performance is reasonable on the XT3 for this benchmark, the limited scalability in the code does not take good advantage of the size and scalability of the XT3 system at ORNL.

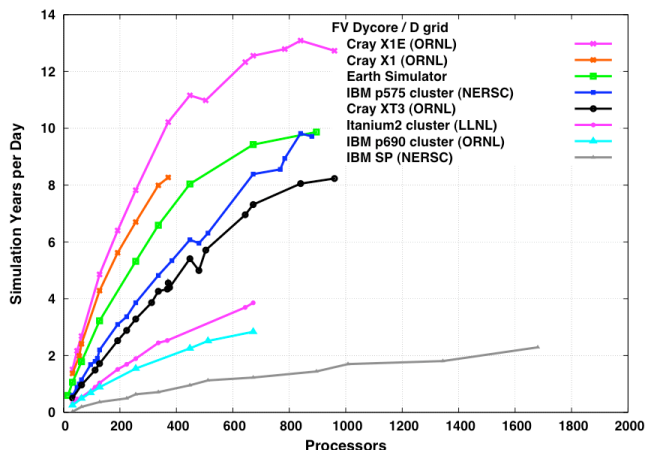


Figure 11: Platform comparisons using CAM D-grid benchmark.

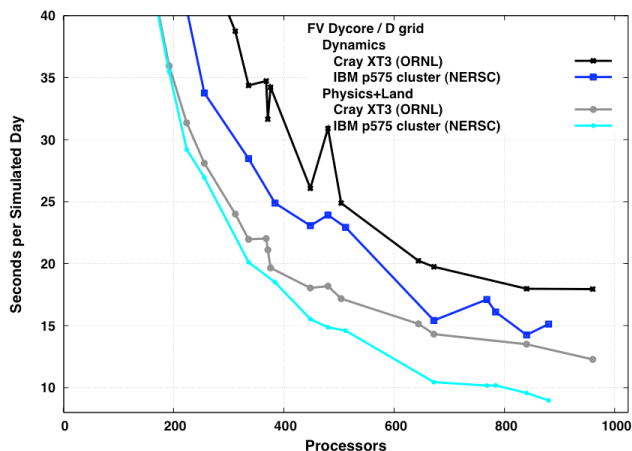
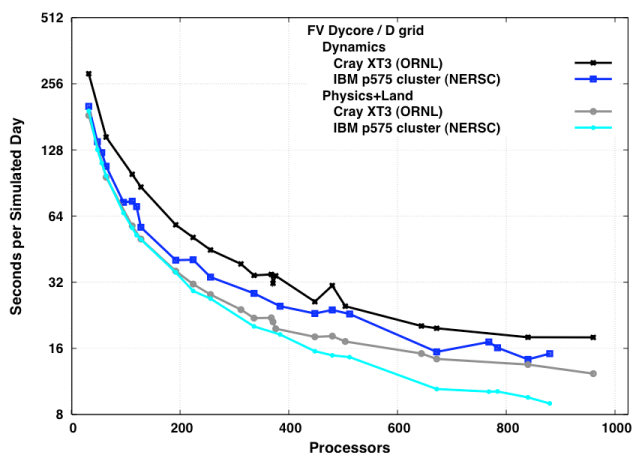


Figure 12: Scaling performance of dynamics and physics for CAM D-grid benchmark.

Figure 11 shows a platform comparison of CAM throughput for the D-grid benchmark problem. The FV dycore supports both a one-dimensional (1D) latitude decomposition and a two-dimensional (2D) decomposition of the computational grid. The 2D decomposition is over latitude and longitude during one phase of the dynamics and over latitude and

vertical in another phase, requiring two remaps of the domain decomposition each timestep. For small processor counts the 1D decomposition is faster than the 2D decomposition, but the 1D decomposition must have at least three latitudes per process and, so, is limited to a maximum of 120 MPI processes for the D-grid benchmark. Using a 2D decomposition requires at least three latitudes and three vertical layers per process, so is limited to  $120 \times 8$ , or 960, MPI processes for the D-grid benchmark. OpenMP can again be used to exploit additional processors. OpenMP is used by the Earth Simulator and the IBM systems, but not by the Cray systems. Each data point in Figure 11 represents the performance on the given platform for the given processor count after optimizing over the available virtual processor grids defining the domain decomposition and after optimizing over the number of OpenMP threads per MPI process. For the D-grid benchmark the XT3 performs significantly better than the Itanium2 cluster and the IBM SP and p690 cluster systems. The XT3 performance lags that of the p575 cluster by 10 to 20 percent.

Figure 12 contains plots of the wallclock seconds per simulation day for the dynamics and for the physics for the XT3 and for the p575 cluster, one with linear-log axes and one with linear-linear axes. The IBM system uses OpenMP to decrease the number of MPI processes, allowing the IBM system to use the 1D domain decomposition in all experiments. The physics costs are identical up through 200 processors. The performance difference between the p575 cluster and the XT3 for larger processor counts is almost entirely due to the runtime difference in computing a global sum and a write to standard out that occurs each timestep. In contrast, dynamics is always faster on the p575, decreasing from a 40% advantage for small processor counts to 25% advantage for large processor counts. The performance difference for large processor counts appears to be due to a higher cost of writes to standard out on the XT3, which increases in relative importance with larger processor counts. For smaller processor counts the reason for the performance difference is not obvious. However the ratio of peak per processor between the XT3 and p575 is 58%, so some of the performance advantage could be due to the processor speed advantage. This is still under investigation.

## 5.2 Parallel Ocean Program (POP)

The Parallel Ocean Program (POP) [26] is the ocean component of CCSM [8] and is developed and maintained at Los Alamos National Laboratory (LANL). The code is based on a finite-difference formulation of the three-dimensional flow equations on a shifted polar grid. In its high-resolution configuration, 1/10-degree horizontal resolution, the code resolves eddies for effective heat transport and the locations of ocean currents.

POP performance is characterized by the performance of two phases: baroclinic and barotropic. The baroclinic phase is three dimensional with limited nearest-neighbor communication and typically scales well on all platforms. In contrast, runtime of the barotropic phase is dominated by the solution of a two-dimensional, implicit system. The performance of the barotropic solver is very sensitive to network latency and typically scales poorly on all platforms.

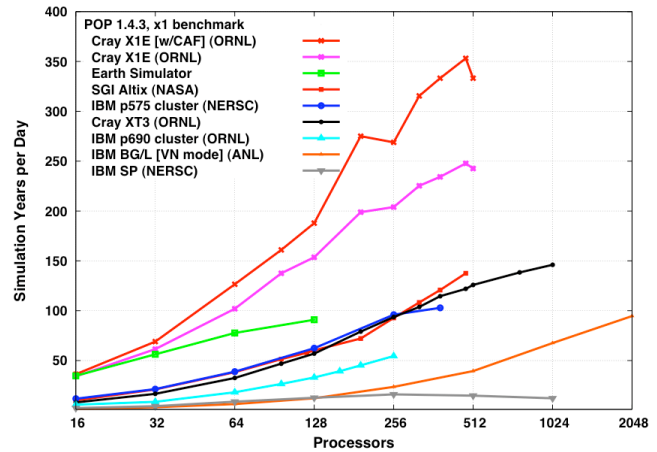


Figure 13: Performance of POP for x1 benchmark.

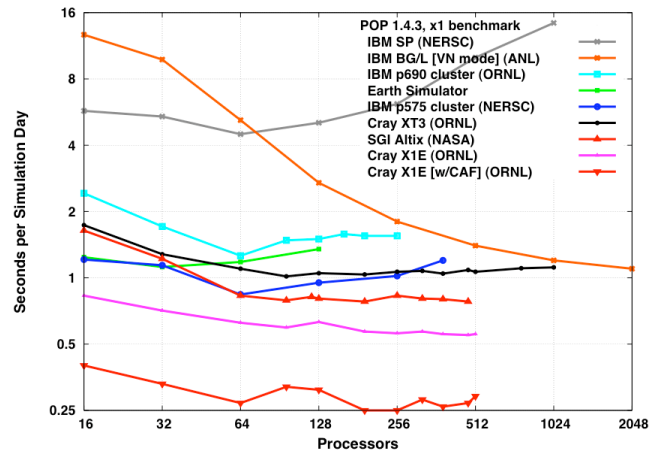


Figure 14: Performance of POP barotropic phase for x1 benchmark.

For our evaluation we used version 1.4.3 of POP and two POP benchmark configurations. The first, referred to as 'x1,' represents a relatively coarse resolution similar to that currently used in coupled climate models. The horizontal resolution is roughly one degree ( $320 \times 384$ ) and uses a displaced-pole grid with the pole of the grid shifted into Greenland and enhanced resolution in the equatorial regions. The vertical coordinate uses 40 vertical levels with smaller grid spacing near the surface to better resolve the surface mixed layer. Because this configuration does not resolve eddies, it requires the use of computationally intensive subgrid parameterizations. This configuration is set up to be identical to the production configuration of the Community Climate

System Model with the exception that the coupling to full atmosphere, ice and land models has been replaced by analytic surface forcing.

Figure 13 shows a platform comparison of POP throughput for the x1 benchmark problem. On the Cray X1E, we considered an MPI-only implementation and also an implementation that uses a Co-Array Fortran (CAF) implementation of a performance-sensitive halo update operation. All other results were for MPI-only versions of POP. The BG/L experiments were run in ‘virtual node’ mode. The XT3 performance is similar to that of both the SGI Altix and the IBM p575 cluster up to 256 processors, and continues to scale out to 1024 processors even for this small fixed size problem.

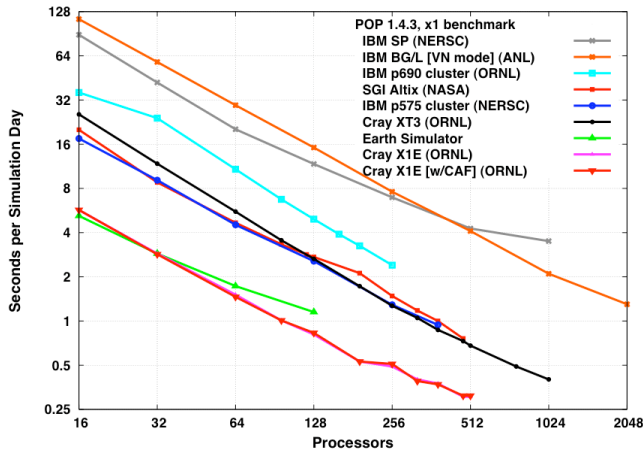


Figure 15: Performance of POP baroclinic phase for x1 benchmark.

Figure 14 shows the performance of the barotropic portion of POP. While lower latencies on the Cray X1E and SGI Altix systems give these systems an advantage over the XT3 for this phase, the XT3 shows good scalability in the sense that the cost does not increase significantly out to 1024 processors. In particular, scaling on the XT3 is superior to that of the p575 cluster and continues to be competitive compared to BG/L. Figure 15 shows the performance of the baroclinic portion of POP. The Cray XT3 performance was very similar to that of both the SGI Altix and the p575 cluster, and shows excellent scalability.

The second benchmark, referred to as ‘0.1,’ utilizes a 1/10-degree horizontal resolution (3600x2400) and 40 vertical levels. The 0.1 degree grid is also a displaced posed grid with 1/10 degree (10km) resolution around the equator down to 2.5km near the poles. The benchmark uses a simple biharmonic horizontal mixing rather than the more expensive subgrid parameterizations used in the x1 benchmark. As mentioned earlier, this resolution resolves eddies for effective heat transport and is used for ocean-only or ocean and sea ice experiments. The cost is prohibitive for use in full coupled climate simulations at the current time.

Figure 16 shows a platform comparison of POP throughput for the 0.1 benchmark. Both performance and scalability on the XT3 are excellent out to almost 5000 processors, achieving 66% efficiency when scaling from 1000 to 5000 processors. Figure 17 shows the performance of both the barotropic and baroclinic phases. From this it is clear that 5000 processors is the practical processor limit on the XT3 as the cost of the barotropic phase dominates that of the baroclinic phase for more than 4000 processors, and is not decreasing. Note that both the X1E and the XT3 demonstrate superlinear speedup in the baroclinic phase, indicating that the problem is still too large to fit into the processor cache even at the maximum processor count. A newer version of POP supports a subblocking technique that should improve cache locality for this benchmark.

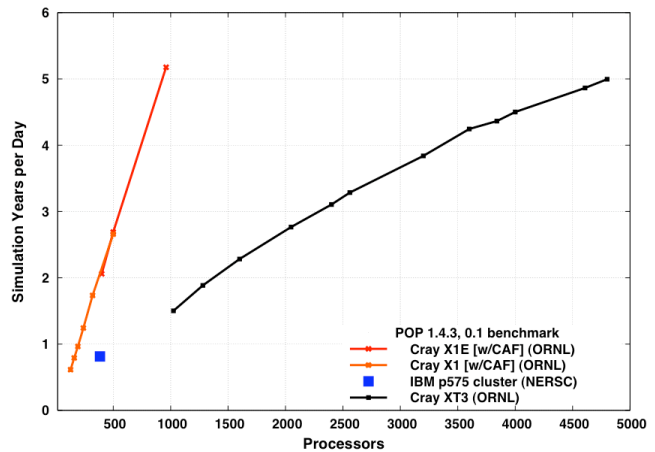


Figure 16: Performance of POP for 0.1 benchmark.

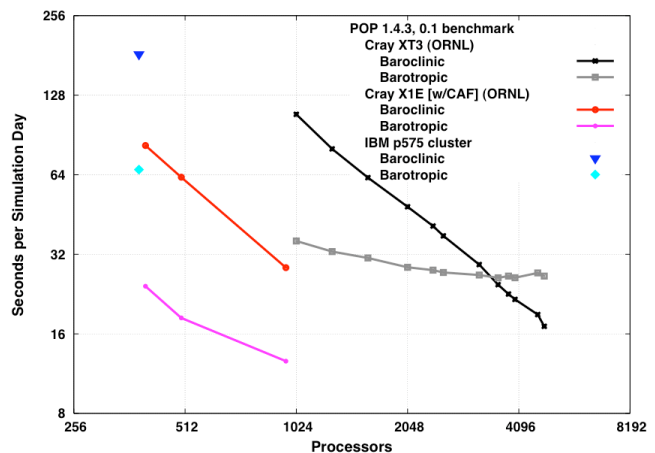


Figure 17: Performance of POP phases for 0.1 benchmark.

### 5.3 GYRO

GYRO [12] is a code for the numerical simulation of tokamak microturbulence, solving time-dependent, nonlinear gyrokinetic-Maxwell equations with gyrokinetic ions and electrons capable of treating finite electromagnetic microturbulence. GYRO uses a

five-dimensional grid and propagates the system forward in time using a fourth-order, explicit Eulerian algorithm. GYRO has been ported to a variety of modern HPC platforms including a number of commodity clusters. Since code portability and flexibility are considered crucial to this code's development team, only a single source tree is maintained and platform-specific optimizations are restricted to a small number of low-level operations such as FFTs. Ports to new architectures often involve nothing more than the creation of a new makefile.

For our evaluation, we ran GYRO version 3.0.0 for two benchmark problems, B1-std and B3-gtc. Newer versions of GYRO are now available that achieve better performance on all platforms. However, we have not had the opportunity to benchmark our test systems using the newer versions of the code. Thus the performance data presented here is a consistent measure of platform capabilities, but not a valid evaluation of current GYRO performance.

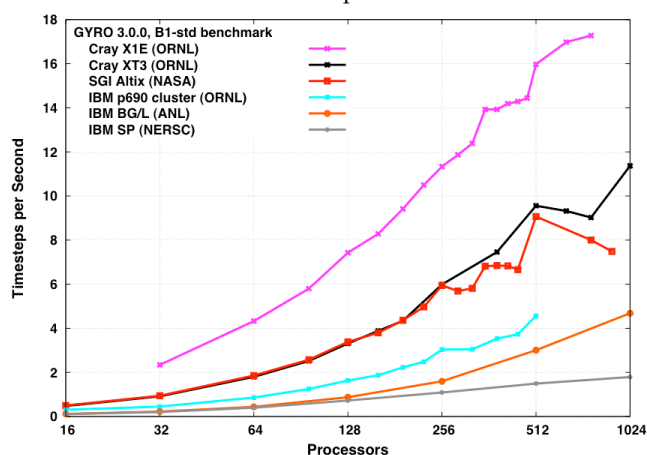


Figure 18: GYRO performance for B1-std benchmark.

B1-std is the Waltz standard case benchmark [44]. This is a simulation of electrostatic turbulence using parameters characteristic of the DIII-D tokamak at mid-radius. Both electrons and ions are kinetic, and electron collisions (pitch-angle scattering) are included. The grid is  $16 \times 140 \times 8 \times 8 \times 20$ . Since 16 toroidal modes are used, a multiple of 16 processors must be used to run the simulation. Interprocess communication overhead for this problem is dominated by the time spent in “transposes” used to change the domain decomposition within each timestep. The transposes are implemented using simultaneous MPI\_Alltoall collective calls over subgroups of processes.

Figure 18 shows platform comparisons of GYRO throughput for the B1-std benchmark problem. Note that there is a strong algorithmic preference for power-of-two numbers of processors for large processor counts, arising from significant redundant work when not using a power-of-two number of processes. This impacts performance differently on the different

systems. The XT3 performance is superior to all of the other platforms except the X1E. Scaling on the XT3 is also excellent out to 512 processors.

Figure 19 plots the ratio of the time spent in the communication transposes to full runtime. The transposes for this problem size are sensitive to both latency and bandwidth. By this metric, the communication performance of the XT3 is among the best compared to the other systems up to 512 processors. The somewhat poor latency on the XT3 degrades this performance metric at higher processor counts compared to the X1E and BG/L.

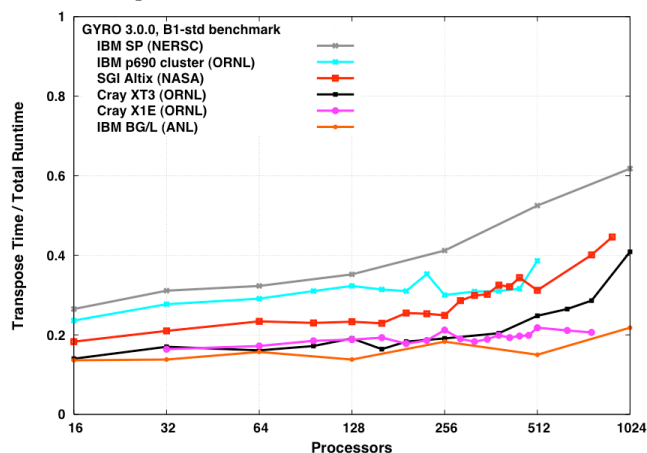


Figure 19: Ratio of time for GYRO transpose communication to total run time for B1-std benchmark.

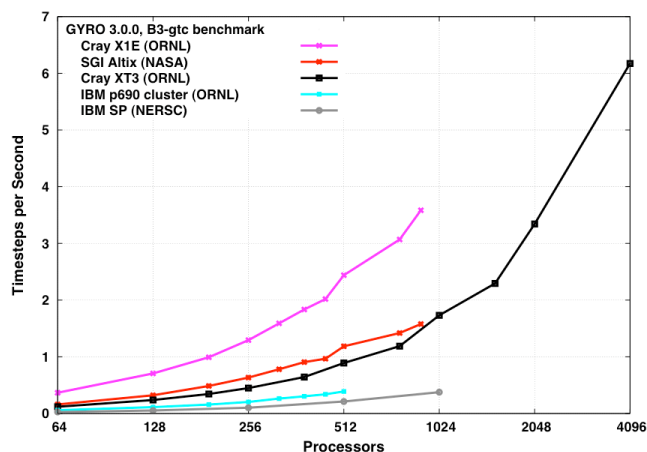


Figure 20: GYRO performance for B3-gtc benchmark.

B3-gtc is a high-toroidal-resolution electrostatic simulation with simplified electron dynamics (only ions are kinetic). The grid is  $64 \times 400 \times 8 \times 8 \times 20$ . This case uses 64 toroidal modes and must be run on multiples of 64 processors. The 400-point radial domain with 64 toroidal modes gives extremely high spatial resolution, but electron physics is ignored, allowing a simple field solve and large timesteps. As with the B1-std benchmark, interprocess communication overhead for this problem is dominated by the time spent in the transposes.

Figure 20 shows platform comparisons of GYRO throughput for the B3-gtc benchmark problem. As with B1-std, there is an algorithmic preference for power-of-two numbers of processors for large processor counts. The Altix is somewhat superior to the XT3 out to 960 processors, but XT3 scalability is excellent, achieving the best overall performance at 4,096 processors.

Figure 21 plots the time spent in the communication transposes for this benchmark. Figure 22 plots the ratio of the time spent in the communication transposes to full runtime. The transposes for this problem size are primarily a measure of communication bandwidth. By these metrics, the communication performance of the XT3 is excellent compared to the other systems, beating even that of the X1E when the relative speed of the rest of the computation is taken into account.

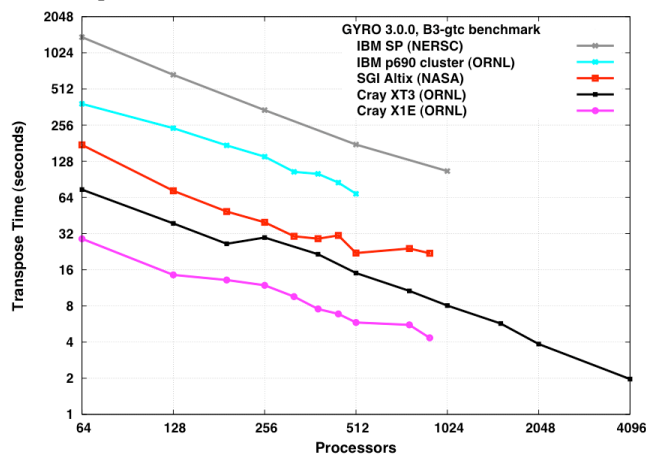


Figure 21: GYRO transpose communication performance for B3-gtc benchmark.

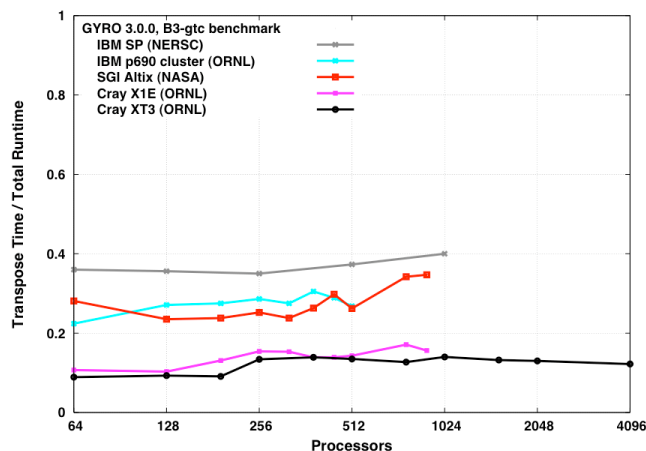


Figure 22: Ratio of GYRO transpose communication time to total run time for B3-gtc benchmark.

## 5.4 S3D

S3D is a code used extensively to investigate first-of-a-kind fundamental turbulence-chemistry interactions in combustion topics ranging from

premixed flames [13, 22], auto-ignition [19], to non-premixed flames [23, 33, 42]. It is based on a high-order accurate, non-dissipative numerical scheme. Time advancement is achieved through a fourth-order explicit Runge-Kutta method, differencing is achieved through high-order (eighth-order with tenth-order filters) finite differences on a Cartesian, structured grid, and Navier-Stokes Characteristic Boundary Conditions (NSCBC) are used to prescribe the boundary conditions. The equations are solved on a conventional structured mesh.

This computational approach is very appropriate for direct numerical simulation of turbulent combustion. The coupling of high-order finite difference methods with explicit Runge-Kutta time integration make very effective use of the available resources, obtaining spectral-like spatial resolution without excessive communication overhead and allowing scalable parallelism.

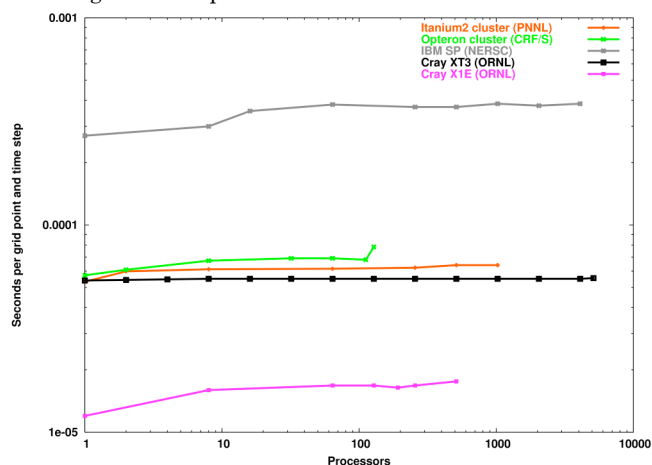


Figure 23: S3D performance.

For our evaluation, the problem configuration is a 3D direct numerical simulation of a slot-burner bunsen flame with detailed chemistry. This includes methane-air chemistry with 17 species and 73 elementary reactions. This simulation used 80 million grid points. The simulation is part of a parametric study performed on different Office of Science computing platforms: the IBM SP at NERSC, the HP Itanium2 cluster at PNNL, and the ORNL Cray X1E and XT3. Figure 23 shows that S3D scales well across the various platforms and exhibited a 90% scaling efficiency on the Cray XT3.

## 5.5 Molecular Dynamics Simulations

Molecular dynamics (MD) simulations enable the study of complex, dynamic processes that occur in biological systems [27]. The MD related methods are now routinely used to investigate the structure, dynamics, functions, and thermodynamics of biological molecules and their complexes. The types of biological activity that has been investigated using MD simulations include protein folding, enzyme catalysation, conformational changes associated with

bimolecular function, and molecular recognition of proteins, DNA, biological membrane complexes. Biological molecules exhibit a wide range of time and length scales over which specific processes occur, hence the computational complexity of an MD simulation depends greatly on the time and length scales considered. With a solvation model, typical system sizes of interest range from 20,000 atoms to more than 1 million atoms; if the solvation is implicit, sizes range from a few thousand atoms to about 100,000. The time period of simulation can range from pico-seconds to the a few micro-seconds or longer.

Several commercial and open source software frameworks for MD calculations are in use by a large community of biologists, including AMBER [37] and LAMMPS [39]. These packages use slightly different forms of potential function and also their own force-field calculations. Some of them are able to use force-fields from other packages as well. AMBER provides a wide range of MD algorithms. The version of LAMMPS used in our evaluation does not use the energy minimization technique, which is commonly used in biological simulations.

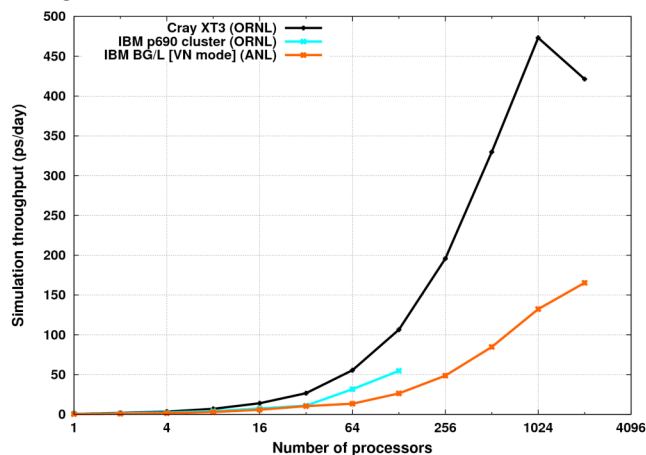


Figure 24: AMBER Simulation Throughput

**AMBER.** AMBER consists of about 50 programs that perform a diverse set of calculations for system preparation, energy minimization (EM), molecular dynamics (MD), and analysis of results. AMBER's main module for EM and MD is known as *sander* (for simulated annealing with NMR-derived energy restraints). We used *sander* to investigate the performance characteristics of EM and MD techniques using the Particle Mesh Ewald (PME) and Generalized Born (GB) methods. We performed a detailed analysis of PME and GB algorithms on massively parallel systems (including the XT3) in other work [3].

The bio-molecular systems used for our experiments were designed to represent the variety of complexes routinely investigated by computational biologists. In particular, we considered the RuBisCO enzyme based on the crystal structure 1RCX, using the Generalized Born method for implicit solvent. The

model consists of 73,920 atoms. In Figure 24, we represent the performance of the code in simulation throughput, expressed as simulation pico-seconds per real day (psec/day). The performance on the Cray XT3 is very good for large-scale experiments, showing a throughput of over twice the other architectures we investigated [3].

**LAMMPS.** LAMMPS (Large-scale Atomic/Molecular Massively Parallel Simulator) [39] is a classical MD code. LAMMPS models an ensemble of particles in a liquid, solid or gaseous state and can be used to model atomic, polymeric, biological, metallic or granular systems. The version we used for our experiments is written in C++ and MPI.

For our evaluation, we considered the RAQ system which is a model on the enzyme RuBisCO. This model consists of 290,220 atoms with explicit treatment of solvent. We observed very good performance for this problem on the Cray XT3 (see Figure 25), with over 60% efficiency on up to 1024 processors and over 40% efficiency on 4096 processor run.

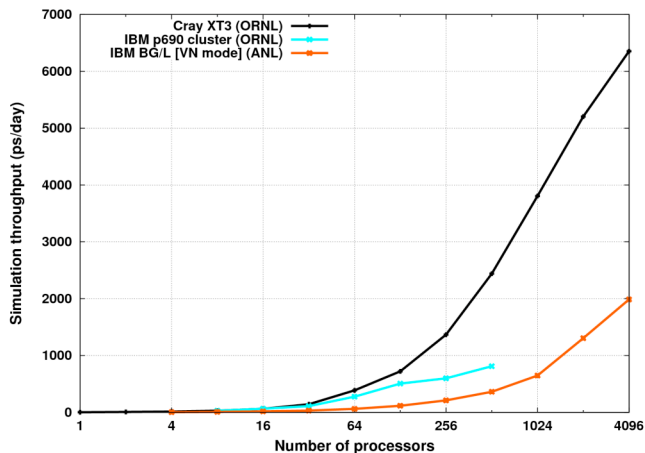


Figure 25: LAMMPS simulation throughput with approximately 290K atoms.

## 5.6 AORSA

The 2- and 3-D all-orders spectral algorithms (AORSA) [25] code is a full-wave model for radio frequency heating of plasmas in fusion devices such as ITER, the international tokamak project. AORSA solves the more general integral form of the wave equation with no restriction on wavelength relative to orbit size and no limit on the number of cyclotron harmonics. With this approach, the limit on attainable resolution comes not from the model, but only from the size and speed of the available computer.

AORSA operates on a spatial mesh, with the resulting set of linear equations solved for the Fourier coefficients. The problem size is characterized by the total number of Fourier modes retained by the model. The physical process is described using a continuous integral equation involving polynomials. The discrete solution must capture the periodic wave behavior,

which is better done using sines and cosines. Application of a fast fourier transform algorithm converts the problem to a frequency space.

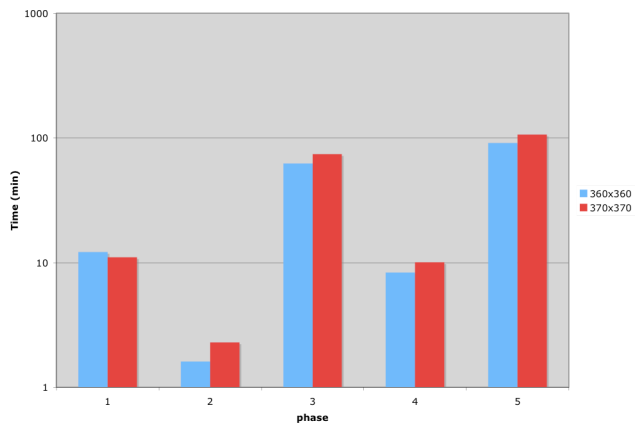
This results in a dense, complex-valued linear system  $A*x=b$ , where  $A$  in  $C^{n \times n}$ ,  $x, b$  in  $C^n$ , that must be solved. This system is solved using the publicly available ScaLAPACK library; in particular routines `pzgetrf` factors the matrix into upper and lower matrices, which `pzgetrs` then uses to compute the solution vector.

Each grid point creates three linear equations, less the point outside of the physical region, so for an  $M \times N$  grid, the linear system is of dimension  $3*M*N - (\sim 30\%)$ . Thus, for example, the  $256 \times 256$  grid creates a linear system of dimension 124,587 and the  $370 \times 370$  grid creates a linear system of dimension 260,226. Immediate plans call for executing across a  $500 \times 500$  grid, which will result in a dense linear system of dimension approaching 500,000.

AORSA is a Fortran parallel processing code developed at Oak Ridge National Laboratory. Code development can be traced back to the 1970's, and thus includes the Fortran definitions and conventions as they were then defined. As the Fortran standard and conventions evolved, the new features were often incorporated into the code base. Thus fixed source, Fortran 77 style code shares space with modern Fortran constructs. In particular, some routines are defined within MODULES, ALLOCATE is used to dynamically manage memory, and KIND adds flexibility for data typing. A modern build system manages ports to several high performance computing platforms. The code base consists of approximately 28,000 lines of executable instructions, 5,500 data declarations, and 8,000 comment lines, contained in around 45 files.

Last summer AORSA was ported to Jaguar, immediately allowing researchers to run experiments at grid resolutions previously unavailable. Up to this point, the finest resolution was  $200 \times 200$ , requiring one hour on 2000 processors on the IBM Power3 Seaborg computer at NERSC. The first large problem run on Jaguar increased the resolution to  $256 \times 256$ , with a runtime of 44.42 minutes on 1024 processors, 27.1 minutes on 2048 processors, and 23.28 on 3072 processors, providing the most detailed simulations ever done of plasma control waves in a tokamak.

Since then experiments using even finer resolutions have been run. For example, preliminary calculations using 4096 processors have allowed the first simulations of mode conversion in ITER. Mode conversion from the fast wave to the ion cyclotron wave (ICW) has been identified in ITER using mixtures of deuterium, tritium and helium3 at 53 MHz.



The above graph shows the performance of various phases of AORSA execution of a simplified version of this problem executed on 4096 processors. The blue bars are timings for the  $360 \times 360$  grid, the red for the  $370 \times 370$  grid. The phases are

- 1) Calculate the Maxwellian matrix.
- 2) Generate and distribute the dense linear system.
- 3) Solve the linear system.
- 4) Calculate the quasi-linear operator.
- 5) Total time.

The ScaLAPACK solver achieves 10.56 TFLOPS, which is about 53% of peak performance. This is in contrast to the LINPACK benchmark result that achieves over 80% of peak performance. We are told that Cray is working on improving the performance of the routines used in AORSA. Further, we are exploring alternative approaches that may reduce runtime.

## 5.7 VH1

VH-1 uses an implementation of the Piecewise Parabolic Method to solve the equations of ideal inviscid compressible fluid flow. It is the primary workhorse for pure hydrodynamics studies undertaken by the SciDAC Terascale Supernova Initiative (TSI), and it also represents an important kernel for several of TSI's multi-dimensional radiation hydrodynamics codes.

Like the ASC benchmark code sPPM, VH-1 is a Lagrangian implementation of PPM and makes use of an Eulerian remap step (However, in contrast to sPPM, the implementation in VH-1 is complete, allowing for the modeling of highly compressible flow like that found in stellar environments). The code uses directional splitting in sweeping through the mesh in the X, Y, and Z directions during each timestep. The current version of the code performs the X and Y sweeps with data in place, then performs a data transpose with a single `MPI_ALLTOALL` before performing the Z sweep. The data is then transposed

back with a second `MPI_ALLTOALL` before the next timestep.

The benchmark problem is a standard Sod shock tube in three dimensions. The benchmark is scaled up with increasing processor count (in keeping with the canonical use of the code), with the total number of zones increasing as the square of the number of processors.

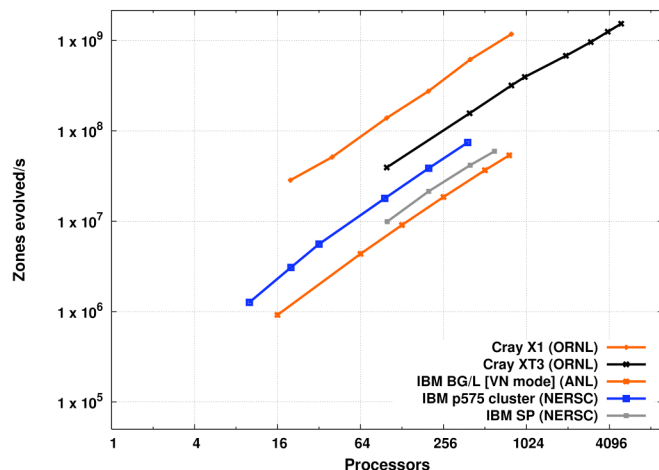


Figure 26: VH-1 performance for 3D Sod shock tube benchmark.

## 5.8 PFLOTRAN

PFLOTRAN (Parallel FLOW and TRANsport) [21, 29, 31, 32, 35] is a state-of-the-art prototype code for modeling multiphase, multicomponent reactive subsurface environmental flows. It is currently being used to understand problems at the Nevada Test Site and the Hanford 300 Area, as well as for geologic CO<sub>2</sub> sequestration studies. The code employs domain-decomposition based parallelism and is built from the ground up using the PETSc framework [5, 6] from Argonne National Laboratory. PFLOTRAN consists of two distinct modules: a flow module (PFLOW) that solves an energy balance equation and mass conservation equations for water and other fluids, and a reactive transport module (PTRAN) that solves mass conservation equations for a multicomponent geochemical system. In coupled mode, flow velocities, saturation, pressure and temperature fields computed from PFLOW are fed into PTRAN. For transient problems, sequential coupling of PFLOW and PTRAN enables changes in porosity and permeability due to chemical reactions to alter the flow field.

Governing equations are discretized using an integral finite-volume formulation on an orthogonal structured grid (extension to unstructured grids is planned). Time-stepping is fully implicit (backward Euler). The nonlinear equations arising at each time step are solved using the Newton-Krylov solver framework of PETSc, allowing easy selection of the most appropriate solvers and preconditioners for the problem at hand.

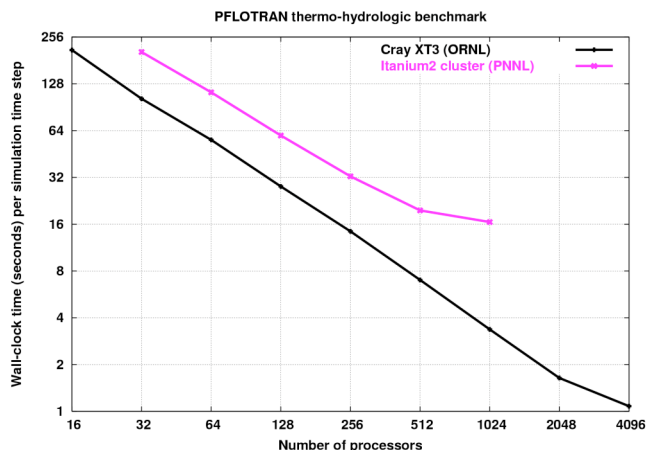


Figure 27: PFLOTRAN performance.

PFLOTRAN has shown excellent parallel scalability. Figure 27 illustrates the performance of the PFLOW module on a modest sized thermo-hydrologic benchmark problem on a 256 x 64 x 256 grid with three degrees of freedom per node (approximately 12.6 million degrees of freedom total). In this case, the linear systems within the Newton method are solved using GMRES(30) with a block-Jacobi pre-conditioner with ILU(0) on each block. The benchmark was run on both the MPP2 Itanium2 cluster (1960 1.5 GHz Itanium2 processors with Quadrics QsNetII interconnect) at PNNL and the Cray XT3 at ORNL. Scaling is exceptionally good on the XT3, with linear speedup on up to 2048 processors, and modest speedup when going to 4096 processors, at which point the modest problem size becomes apparent and the numerous MPI Reductions inside the linear system solver present a scalability barrier. Since reactive flow problems for production runs will often involve 10-20 chemical degrees of freedom per node, we expect to see even better parallel efficiency for problems involving reactive chemistry.

## 6 Conclusions and Plans

Oak Ridge National Laboratory has received and installed a 5,294 processor Cray XT3. In this paper we describe our performance evaluation of the system as it was being deployed, including micro-benchmark, kernel, and application benchmark results. We focused on applications from important Department of Energy applications areas including climate and fusion. In experiments with up to 4096 processors, we observed that the Cray XT3 shows tremendous potential for supporting the Department of Energy application workload, with good scalar processor performance and high interconnect bandwidth when compared to other microprocessor-based systems.

## Acknowledgements

This research was sponsored by the Office of Mathematical, Information, and Computational Sciences, Office of Science, U.S. Department of Energy under Contract No. DE-AC05-00OR22725 with UT-Battelle, LLC. Accordingly, the U.S. Government retains a non-exclusive, royalty-free license to publish or reproduce the published form of this contribution, or allow others to do so, for U.S. Government purposes.

Also, we would like to thank Jeff Beckleheimer, John Levesque, Nathan Wichmann, and Jim Schwarzmeier of Cray, and Don Maxwell of ORNL for all their assistance in this endeavor.

We gratefully acknowledge Jeff Kuehn of ORNL for collection of performance data on the BG/L system; Hongzhang Shan of LBL for collecting GYRO performance data on the IBM SP; James B. White III for collecting POP performance data on the p575 cluster; Yoshikatsu Yoshida for collecting POP performance data on the Earth Simulator; David Parks for collecting CAM performance data on the Earth Simulator; Michael Wehner for collecting CAM performance data on the IBM SP; and Arthur Mirin for collecting CAM performance data on the Itanium2 cluster at LLNL. We thank the National Energy Research Scientific Computing Center for access to the IBM SP, Argonne National Laboratory for access to the IBM BG/L, the NASA Advanced Supercomputing Division for access to their SGI Altix, and the ORNL Center for Computational Sciences (CCS) for access to the Cray X1, Cray X1E, Cray XD1, Cray XT3, IBM p690 cluster, and SGI Altix. The CCS is supported by the Office of Science of the U.S. Department of Energy under Contract No. DE-AC05-00OR22725.

## References

- [1] *Community Climate System Model*, <http://www.cesm.ucar.edu/>.
- [2] P.A. Agarwal, R.A. Alexander *et al.*, "Cray X1 Evaluation Status Report," ORNL, Oak Ridge, TN, Technical Report ORNL/TM-2004/13, 2004, <http://www.csm.ornl.gov/evaluation/PHOENIX/PDF/CRAYEvaluationTM2004-15.pdf>.
- [3] S.R. Alam, P. Agarwal *et al.*, "Performance Characterization of Molecular Dynamics Techniques for Biomolecular Simulations," Proc. ACM SIGPLAN Symposium on Principles and Practice of Parallel Programming (PPOPP), 2006.
- [4] AMD, "Software Optimization Guide for AMD Athlon™ 64 and AMD Opteron™ Processors," Technical Manual 25112, 2004.
- [5] S. Balay, K. Buschelman *et al.*, "PETSc Users Manual," Argonne National Laboratory 2004.
- [6] S. Balay, K. Buschelman *et al.*, *PETSc Web page*, 2001.
- [7] M.B. Blackmon, B. Boville *et al.*, "The Community Climate System Model," *BAMS*, 82(11):2357-76, 2001.
- [8] M.B. Blackmon, B. Boville *et al.*, "The Community Climate System Model," *BAMS*, 82(11):2357-76, 2001.
- [9] R. Brightwell, W. Camp *et al.*, "Architectural Specification for Massively Parallel Computers-An Experience and Measurement-Based Approach," *Concurrency and Computation: Practice and Experience*, 17(10):1271-316, 2005.
- [10] R. Brightwell, L.A. Fisk *et al.*, "Massively Parallel Computing Using Commodity Components," *Parallel Computing*, 26(2-3):243-66, 2000.
- [11] R. Brightwell, R. Riesen *et al.*, "Portals 3.0: Protocol Building Blocks for Low Overhead Communication," Proc. Workshop on Communication Architecture for Clusters (in conjunction with International Parallel & Distributed Processing Symposium), 2002, pp. 164-73.
- [12] J. Candy and R. Waltz, "An Eulerian gyrokinetic-Maxwell solver," *J. Comput. Phys.*, 186(545), 2003.
- [13] J.H. Chen and H.G. Im, "Stretch effects on the Burning Velocity of turbulent premixed hydrogen-Air Flames," Proc. Comb. Inst, 2000, pp. 211-8.
- [14] W.D. Collins and P.J. Rasch, "Description of the NCAR Community Atmosphere Model (CAM 3.0)," National Center for Atmospheric Research, Boulder, CO 80307 2004.
- [15] W.D. Collins, P.J. Rasch *et al.*, "The Formulation and Atmospheric Simulation of the Community Atmosphere Model: CAM3," *Journal of Climate*, to appear, 2006.
- [16] L. Dagum and R. Menon, "OpenMP: : An Industry-Standard API for Shared-Memory Programming," *IEEE Computational Science & Engineering*, 5(1):46--55, 1998.
- [17] T.H. Dunigan, Jr., J.S. Vetter *et al.*, "Performance Evaluation of the Cray X1 Distributed Shared Memory Architecture," *IEEE Micro*, 25(1):30-40, 2005.
- [18] T.H. Dunigan, Jr., J.S. Vetter, and P.H. Worley, "Performance Evaluation of the SGI Altix 3700," Proc. International Conf. Parallel Processing (ICPP), 2005.
- [19] T. Echehki and J.H. Chen, "Direct numerical simulation of autoignition in non-homogeneous hydrogen-air mixtures," *Combust. Flame*, 134:169-91, 2003.
- [20] M.R. Fahey, S.R. Alam *et al.*, "Early Evaluation of the Cray XD1," Proc. Cray User Group Meeting, 2005, pp. 12.
- [21] G.E. Hammond, A.J. Valocchi, and P.C. Lichtner, "Application of Jacobian-free Newton-Krylov with physics-based preconditioning to biogeochemical

- transport,” *Advances in Water Resources*, 28:359-76, 2005.
- [22] E.R. Hawkes and J.H. Chen, “Direct numerical simulation of hydrogen-enriched lean premixed methane-air flames,” *Combust. Flame*, 138(3):242-58, 2004.
- [23] E.R. Hawkes, R. Sankaran *et al.*, “Direct numerical simulation of turbulent combustion: fundamental insights towards predictive models,” Proc. SciDAC PI Meeting, 2005.
- [24] High-End Computing Revitalization Task Force (HECRTF), “Federal Plan for High-End Computing,” Executive Office of the President, Office of Science and Technology Policy, Washington, DC 2004.
- [25] E.F. Jaeger, L.A. Berry *et al.*, “????,” *Phys. Plasmas*, 8(1573), 2001.
- [26] P.W. Jones, P.H. Worley *et al.*, “Practical performance portability in the Parallel Ocean Program (POP),” *Concurrency and Computation: Experience and Practice*(in press), 2004.
- [27] M. Karplus and G.A. Petsko, “Molecular dynamics simulations in biology,” *Nature*, 347, 1990.
- [28] J.T. Kiehl, J.J. Hack *et al.*, “The National Center for Atmospheric Research Community Climate Model: CCM3,” *Journal of Climate*, 11:1131-49, 1998.
- [29] P.C. Lichtner and A. Wolfsberg, “Modeling Thermal-Hydrological-Chemical (THC) Coupled Processes with Applications to Underground Nuclear Tests at the Nevada Test Site; A Grand Challenge Supercomputing Problem,” Proc. MPU Workshop: Conceptual Model Development for Subsurface Reactive Transport Modeling of Inorganic Contaminants, Radionuclides and Nutrients, 2004.
- [30] S.J. Lin, “A vertically Lagrangian finite-volume dynamical core for global models,” *MWR*, 132(10):2293--307, 2004.
- [31] C. Lu and P.C. Lichtner, “PFLOTRAN: Massively Parallel 3-D Simulator for CO<sub>2</sub> Sequestration in Geologic Media,” in *DOE-NETL Fourth Annual Conference on Carbon Capture and Sequestration*, 2005
- [32] C. Lu, P.C. Lichtner *et al.*, “Parametric study of CO<sub>2</sub> sequestration in geologic media using the massively parallel computer code PFLOTRAN,” Proc. AGU Fall Meeting, 2005.
- [33] S. Mahalingam, J.H. Chen, and L. Vervisch, “Finite-rate chemistry and transient effects in direct numerical simulations of turbulent non-premixed flames,” *Combust. Flame*, 102(3):285-97, 1995.
- [34] T.G. Mattson, D. Scott, and S.R. Wheat, “A TeraFLOP Supercomputer in 1996: The ASCI TFLOP System,” Proc. 10th International Parallel Processing Symposium (IPPS 96), 1996, pp. 84-93.
- [35] R.T. Mills, P.C. Lichtner, and C. Lu, “PFLOTRAN: A massively parallel simulator for reactive flows in geologic media (poster),” in *SC2005*, 2005
- [36] P.J. Mucci, K. London, and J. Thurman, “The CacheBench Report,” University of Tennessee, Knoxville, TN 1998.
- [37] D.A. Pearlman, D.A. Case *et al.*, “AMBER, a package of computer programs for applying molecular mechanics, normal mode analysis, molecular dynamics and free energy calculations to simulate the structural and energetic properties of molecules,” *Computer Physics Communication*, 91, 1995.
- [38] K. Pedretti, R. Brightwell, and J. Williams, “Cplant Runtime System Support for Multi-Processor and Heterogeneous Compute Nodes,” Proc. IEEE International Conference on Cluster Computing (CLUSTER 2002), 2002, pp. 207-14.
- [39] S.J. Plimpton, “Fast Parallel Algorithms for Short-Range Molecular Dynamics,” in *Journal of Computational Physics*, vol. 117, 1995
- [40] S.L. Scott, “Synchronization and Communication in the T3E Multiprocessor,” Proc. Architectural Support for Programming Languages and Operating Systems (ASPLOS), 1996, pp. 26-36.
- [41] M. Snir, W.D. Gropp *et al.*, Eds., *MPI-the complete reference (2-volume set)*, 2nd ed. Cambridge, Mass.: MIT Press, 1998.
- [42] J.C. Sutherland, P.J. Smith, and J.H. Chen, “Quantification of Differential Diffusion in Nonpremixed Systems,” *Combust. Theory and Modelling (to appear)*, 2005.
- [43] US Department of Energy Office of Science, “A Science-Based Case for Large-Scale Simulation,” US Department of Energy Office of Science 2003, <http://www.pnl.gov/scales>.
- [44] R.E. Waltz, G.R. Kerbel, and J. Milovich, “Toroidal gyro-Landau fluid model turbulence simulations in a nonlinear ballooning mode representation with radial modes,” *Phys. Plasmas*, 1:2229, 1994.
- [45] D.L. Williamson and J.G. Olson, “Climate simulations with a semi-Lagrangian version of the NCAR Community Climate Model,” *MWR*, 122:1594-610, 1994.
- [46] P.H. Worley, “CAM Performance on the X1E and XT3,” Proc. Proceedings of the 48th Cray User Group Conference, May 8-11, 2006, 2006.